Rapid warming events in a small coastal upwelling embayment

A Senior Project
presented to
the Faculty of the Physics Department
California Polytechnic State University – San Luis Obispo

In Fulfillment
of the Requirements for the Degrees
Bachelor of Science in Computer Science and
Bachelor of Science in Marine Science

By

Tatjana E. Ellis

June 2021

Approval Page

Title: Rapid warming events in a small coastal upwelling embayment

Author: Tatjana E. Ellis

Date Submitted: 06/11/2021

Senior Thesis Advisor: Dr. Ryan K. Walter

_____

Signature

_____

Date

1 Introduction

Understanding nearshore temperature variability is critical for a range of biological, chemical, and physical processes. Temperature can be used as a general indicator of environmental conditions and water mass characteristics, since changes in temperature are often correlated with changes in nutrients and other biogeochemical parameters (Lucas et al. 2011, Chavez et al. 2011, Booth et al. 2012, Walter et al. 2018). Temperature conditions have also been shown to drive larval connectivity patterns and habitat ranges (O'Connor et al. 2007). Additionally, rapid temperature changes and their range can significantly impact nearshore ecosystems and ecology, such as influencing the severity of coral bleaching (Safaie et al. 2017), or regulating organismal attributes, including larval development rate, survival, and overall population connectivity and community structure (O'Connor et al. 2007). Finally, a better understanding of nearshore temperature variability will be critical in reducing uncertainty in the coastal ocean response to future climate change.

In eastern boundary currents, coastal temperature variability is driven by a host of physical processes on various spatial and temporal scales. These include seasonal upwelling (Walter et al. 2018, Garcia-Reyes and Largier 2012), upwelling-relaxation cycles (Walter et al. 2017), warm water poleward flows during relaxation events (the period between upwelling events; Washburn et al. 2011), internal waves and bores (Walter et al. 2012, 2014), persistent coastal fronts (Walter et al. 2016), coastal plumes such as outfalls and rivers (Wolanski et al. 1984), and mesoscale and submesoscale features such as eddies and filaments (Nidzieko and Largier 2013). In coastal embayments, variable coastline orientation and the presence of topographic features can alter nearshore temperature dynamics substantially through the modulation of upwelling forcing (Largier, 2020). In some systems, upwelling shadows develop, whereby regional upwelling forcing

inside the bay is sheltered, leading to a system with warmer water and increased residence times relative to outside the bay, creating local hotspots for harmful algal blooms and hypoxia risk (Walter et al. 2018, Barth et al. 2020, Largier 2020, Valera et al. 2020). Despite recent progress (cf. Largier 2020 and the references therein), there are still significant gaps in the understanding of drivers of temperature variability in upwelling bays, with important implications for ecosystem response.

In this contribution, we investigate nearshore temperature variability in a small upwelling shadow bay in Central California [San Luis Obispo (SLO) bay], located near a major marine biogeographic boundary (Point Conception). Specifically, we investigate fast time-scale (O(hours), see Nidzieko and Largier 2013 and their description of warm-water intrusions at a nearby site) warming events, and their climatology, using a decade of nearshore measurements both inside and outside the bay. We also incorporate remotely sensed satellite data, to attempt to determine their source and dynamics. Finally, we compare these warm-water intrusion events, and their climatology, inside and outside of the upwelling shadow bay to better understand the influence of the upwelling shadow on temperature variability at this site. Implications of the results are discussed.

2 Data and Methods

2.1 Site Description

San Luis Obispo (SLO) Bay is a small, semi-enclosed coastal embayment on the central California coast along the eastern Pacific Ocean. The northern portion of SLO Bay is enclosed and sheltered by coastal peaks and topographic features (**Figure 1**). SLO Bay is home to considerable ecological diversity (including giant kelp forests), a major fishing port (Port San Luis), popular

beaches (e.g. Pismo Beach, Avila Beach, etc.), many tourist destinations, and the California Polytechnic State University (Cal Poly) Pier. SLO Bay is also subject to frequent harmful algal blooms (Barth et al. 2020) and hypoxic events (Valera et al. 2020).

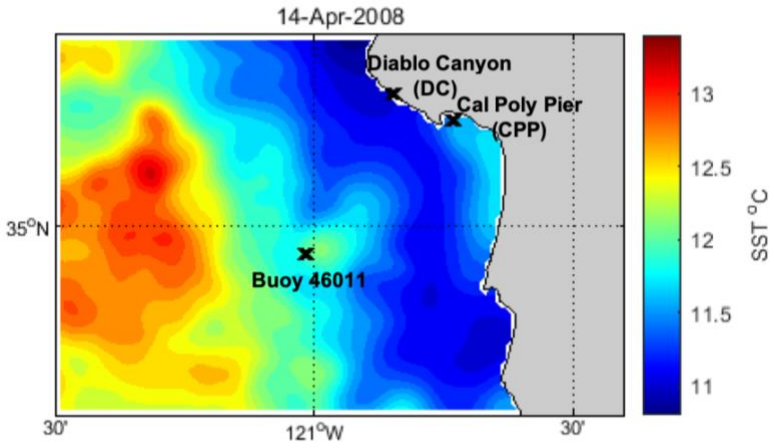

Figure 1. San Luis Obispo Bay study region highlighting the locations of data used in the analysis. Shown also is the MUR SST from April 14th, 2008.

2.2 Upwelling Wind Data

To calculate the upwelling winds off the coast of Cal Poly Pier, we used wind data collected by the National Data Buoy Center (NDBC) at buoy 46011. Details about this station can be found at https://www.ndbc.noaa.gov/station_page.php?station=46011. Wind data were rotated to 150° from true north, such that winds parallel to the coast and equatorward (upwelling favorable) are positive and winds oriented poleward (downwelling favorable) are negative. We denote upwelling events when the upwelling favorable wind exceeds 5 m/s (Paduan et al. 2018). Winds were low pass filtered (33 hr) to isolate the role of low-frequency variability (e.g., upwelling/relaxation cycles).

2.3 Temperature Data

2.3.1 Data

Temperature data from inside the bay at the Cal Poly Pier (CPP) used in this analysis were collected by a profiling CTD (Conductivity, Temperature, Depth) instrument on the end of the CPP (see **Figure 1**). This CTD has been collecting data continuously from 2005 to present, by automatically lowering to the bottom of the ocean (approximately 9 m deep), and collecting data profiles along the way while sampling at 1 Hz. These profiles are collected every 30 minutes. More details about this profiler are described in Walter et al. (2018), and data access can be found at https://www.cencoos.org/observations/sensor-platforms/shore-stations/.

To investigate differences between inside and outside the bay, data from outside of the coastal embayment were also analyzed (hereafter DC for Diablo Canyon). These data were collected at a fixed site in approximately 3 m of water just south of the Diablo Canyon nuclear power plant (see **Figure 1**). This site is located outside of the discharge outfall region, such that the temperatures collected are not influenced by the nearby nuclear power plant thermal discharge. These data are also described in more detail in Walter et al. (2018).

Data from 3 m and 5 m depths were considered at the CPP site for comparison with DC. Data from the 5m depth at CPP typically tracked the trends found at lower depths at CPP.

2.3.2. Data Processing

For comparison, DC data were first interpolated to the time series data from CPP. Next, a 33-hr low-pass filter was applied to both the CPP and DC datasets, thereby removing higher frequency variability associated with tides and local diurnal winds (e.g., Walter et al. 2017). Last, all missing time points in one dataset were removed from the others for comparative statistics. The full resulting datasets are shown in **Figure 2**.

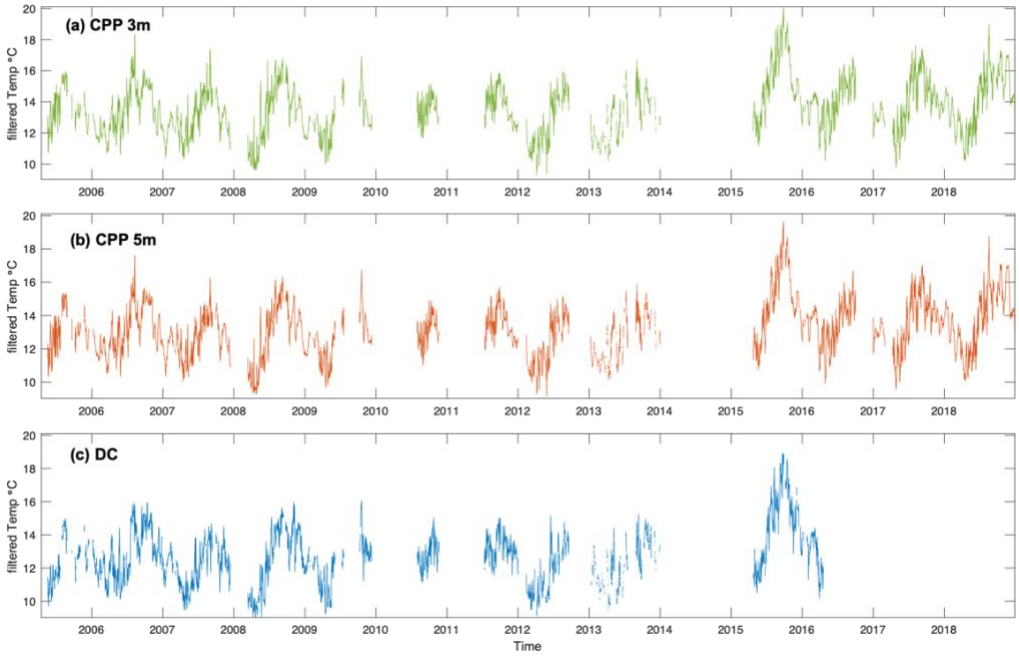

Figure 2. Available temperature data from 2005 to 2019 at (a) Cal Poly Pier 3m depth, (b) Cal Poly Pier 5m depth, and (c) Diablo Canyon 3m depth.

2.3.3. Intrusion events

A rapid warming event (or interchangeably described as warm-water intrusion events following Nidzieko and Largier (2013)) is defined as a period of time over which the change in temperature with time is above a given threshold for at least 3 hrs, without any missing data within the interval. To determine this, we first numerically calculated the derivative of the low-pass filtered temperature with respect to time (dT/dt), or effectively an instantaneous warming rate, and then find all instances above a given threshold. If the instance met the requirements, being at least 3 hours long and providing continuous data within the interval, it was stored as a potential intrusion event. These events were calculated using various thresholds, ranging from 0.03 to 0.09 ^{o}C/hr. A lower threshold of 0.03 ^{o}C/hr was used following the analysis by Nidzieko & Largier (2013) and Melton et al. (2009). We also quantified the events greater than this threshold (up to 0.09 ^{o}C/hr) to quantify more extreme warming events.

To determine the seasonality of these rapid warming events, we also calculated the average number of events per month. This was done by counting the total number of events found per month across all the years where data were available for all three datasets, and then dividing by the total number of data points available for each month. This resulted in the average across all data available for each dataset, while also accounting for the missing data points across the years.

We also examined and detailed the ten largest rapid warming events recorded. These were defined as the events at CPP 3 m depth with the largest change in temperature over the entire event interval.

2.4 Satellite Sea Surface Temperature (SST) Data

Since the temperature data at CPP and DC are both at fixed locations, we also used satellite sea surface temperature (SST) data to get a better idea of the spatial evolution of each rapid warming event. This allowed for a more detailed understanding of what mechanism or processes might be driving potential intrusion events, the spatial scale at which these warming events occur, and a better understanding of differences in warming inside versus outside the bay. For this, we used data from two different satellites.

The first product we used was the National Oceanic and Atmospheric Administration's Polar Orbiting Environmental Satellite (NOOA POES) with the Advanced Very High Resolution Radiometer (AVHRR). Compared to several other products (e.g., Aqua and Terra MODIS), this product provided the best resolution and most consistent data coverage in our domain. AVHRR data better resolved small-scale, local SST features and gradients, due to its high spatial resolution (0.0125 degrees). However, this product still had periods with missing data, likely due to cloud cover. The Level 3 data product, with a 1-day composite as used in our analysis, is described and

can be publically accessed and visualized on the NOAA Coast Watch website[1], or directly accessed from the CeNCOOS THREDDS data server[2].

The other product used was a level 4 blended product called the Multi-scale Ultra High Resolution (MUR) SST, which blends multiple satellites, resulting in more data availability both spatially and temporally. However, it has the disadvantage of smoothing out large gradients that may be dynamically relevant, including sharp fronts and some submesoscale features like filaments and eddies. The MUR SST blended product is described and can be publically accessed and visualized on the NOAA Coast Watch website[3], or the data can be directly accessed in OPeNDAP format[4].

3 Results

3.1 Rapid warming event climatology

The average number of rapid warming events across multiple thresholds showed a noticeable seasonal trend at the Cal Poly Pier (CPP), both at 3 m and 5 m depths, with a large increase in events during summer months, especially May to August (**Figure 3**). CPP 3m depth had more events at lower thresholds compared to 5m depth, but had less events at higher thresholds (i.e., > 0.07 ^{o}C/hr) (**Table 1, Figure 3**). Diablo Canyon (DC), compared with CPP, had significantly less warming events overall, and did not exhibit as much of a seasonal trend. Instead, events were observed throughout the year, with no large increase in summer months. However,

[1] https://coastwatch.pfeg.noaa.gov/erddap/griddap/erdATssta1day_LonPM180.graph
[2] http://thredds.cencoos.org/thredds/catalog.html?dataset=ERDATSSTA1DAY
[3] https://coastwatch.pfeg.noaa.gov/erddap/griddap/erdMurFront41USWest.graph?.colorBar=Rainbow
[4] https://podaac-opendap.jpl.nasa.gov/opendap/allData/ghrsst/data/GDS2/L4/GLOB/JPL/MUR/v4.1/

winter months, primarily December to February, exhibited a small number of events compared to the rest of the year.

Table 1. Average statistics of all rapid warming events captured at Cal Poly Pier 3 m depth, 5 m depth, and Diablo Canyon 3m depth from thresholds of 0.03 to 0.09 ºC/hr in intervals of 0.02 ºC/hr from 2005 to 2015.

Threshold	Dataset	Total # events	Average ΔT (°C) of events		Average Δt (hrs) of events	
			Mean	Standard deviation	Mean	Standard deviation
0.03	**CPP 3m**	396	0.73	0.54	15.53	7.82
	CPP 5m	375	0.79	0.56	15.75	7.18
	DC	293	0.70	0.53	15.40	8.20
0.05	**CPP 3m**	182	0.78	0.54	12.09	5.82
	CPP 5m	196	0.85	0.54	12.66	5.08
	DC	120	0.74	0.53	11.87	5.70
0.07	**CPP 3m**	70	0.87	0.54	10.46	4.35
	CPP 5m	91	0.90	0.58	10.64	4.64
	DC	44	0.79	0.58	9.95	5.22
0.09	**CPP 3m**	27	0.95	0.57	9.52	4.06
	CPP 5m	39	0.95	0.62	9.46	4.01
	DC	15	0.90	0.64	9.27	5.13

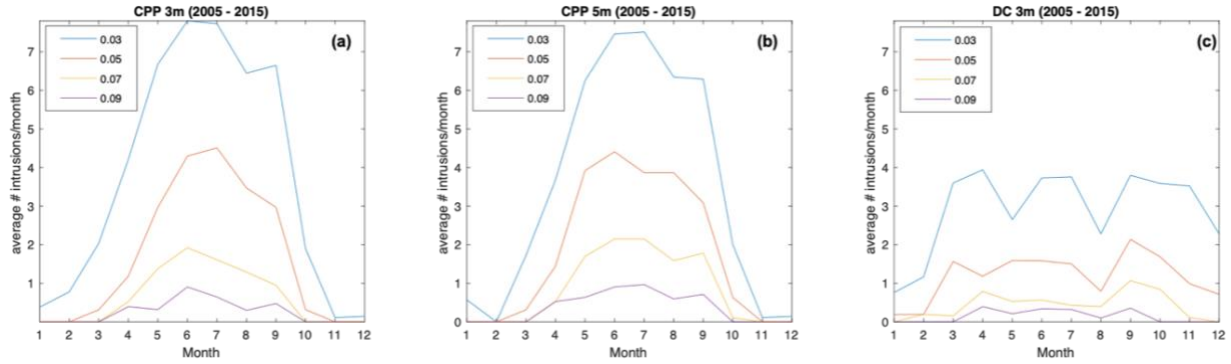

Figure 3. Average number of potential intrusions per month over the years 2005 to 2015 at cutoff thresholds from 0.03 ºC/hr to 0.9 ºC/hr in intervals of 0.02 ºC/hr from the (a) Cal Poly Pier 3 m depth, (b) Cal Poly Pier 5 m depth, and (c) Diablo Canyon 3 m depth.

Overall, trends and seasonality were robust across all different thresholds tested here. And, as expected, there were progressively more warming events delineated for lower warming thresholds. For example, a threshold of 0.03 ºC/hr, as used by Nidzieko and Largier (2013), captured more events, including several with smaller rates of warming. For a threshold of 0.07 ºC/hr, CPP 5 m had the most events with the highest mean change in temperature, and the highest mean duration of events (**Table 1**). On the contrary, DC had the lowest values for the mean change

in temperature and mean duration. However, notably, CPP 3 m exhibited the lowest standard deviations for all metrics.

Additionally, comparing the summary statistics for all thresholds tested, CPP 3m depth initially captured more events than 5m depth at a lower threshold of 0.03 ºC/hr, which was not true as the threshold increased above 0.05 ºC/hr (**Table 1**). DC consistently exhibited the lowest number of events captured across all thresholds. As expected, the mean change in temperature increased, and the mean duration decreased, as the threshold increased. Standard deviations for the average change in temperature only increased slightly with increasing threshold, while the standard deviations of the average durations noticeably decreased with increasing threshold.

3.2 Extreme rapid warming events

Three of the top ten largest rapid warming events based on CPP 3m depth at a threshold of 0.07 ºC/hr (events 2, 5, and 9) had no DC data available, as the DC data were only available through mid-2016 (**Table 2**, **Figure 2**). For this reason, these three events were not used for our comparison. Out of the seven events where DC data were available, only two events also displayed warming rates above the 0.07 ºC/hr threshold at DC, indicating the largest rapid warming events occurred exclusively inside the bay. Notably, all of the events occurred between April and September, during the major upwelling season (Walter et al. 2018). Changes in temperature at CPP 3m ranged from 1.46 – 2.65 ºC with durations from 15 to 21 hrs, and exhibited max warming rates between 0.12 and 0.17 ºC/hr. Additionally, 9 of the 10 events observed at CPP 3 m were also observed at 5 m depth, except for event 10.

Table 2. Top ten rapid warming events based on the largest change in temperature (ΔT) at Cal Poly Pier 3 m depth with a threshold of 0.07 ºC/hr between 2005 and 2015. NA indicates no data were available for this date.

Event #	Start Date (DD-MM-YYYY)		CPP 3m	CPP 5m	DC
1	13-04-2008	dT/dt max (°C/hr)	**0.17**	**0.20**	0.00
		ΔT (°C)	**2.65**	**2.97**	-0.03
		Δt (hrs)	**20**	**20**	20
2	21-07-2018	dT/dt max (°C/hr)	**0.17**	**0.21**	NA
		ΔT (°C)	**2.45**	**3.14**	NA
		Δt (hrs)	**19**	**20**	NA
3	20-07-2006	dT/dt max (°C/hr)	**0.12**	**0.10**	**0.13**
		ΔT (°C)	**2.06**	**1.75**	**2.24**
		Δt (hrs)	**21**	**21**	**21**
4	02-09-2013	dT/dt max (°C/hr)	**0.12**	**0.13**	0.00
		ΔT (°C)	**1.80**	**1.81**	-0.29
		Δt (hrs)	**18**	**17**	18
5	25-05-2017	dT/dt max (°C/hr)	**0.13**	**0.12**	NA
		ΔT (°C)	**1.76**	**2.01**	NA
		Δt (hrs)	**17**	**20**	NA
6	03-09-2010	dT/dt max (°C/hr)	**0.12**	**0.11**	-0.02
		ΔT (°C)	**1.71**	**1.65**	-0.46
		Δt (hrs)	**17**	**18**	17
7	15-05-2008	dT/dt max (°C/hr)	**0.12**	**0.10**	0.05
		ΔT (°C)	**1.64**	**1.45**	0.40
		Δt (hrs)	**17**	**17**	17
8	27-04-2008	dT/dt max (°C/hr)	**0.12**	**0.11**	0.01
		ΔT (°C)	**1.62**	**1.18**	0.09
		Δt (hrs)	**17**	**13**	17
9	11-08-2018	dT/dt max (°C/hr)	**0.13**	**0.14**	NA
		ΔT (°C)	**1.59**	**2.02**	NA
		Δt (hrs)	**15**	**18**	NA
10	11-06-2008	dT/dt max (°C/hr)	**0.12**	0.06	**0.08**
		ΔT (°C)	**1.46**	0.74	**0.44**
		Δt (hrs)	**15**	15	**7**

To examine a few of these events in more detail, we examined events 1 (**Figure 4**), 3 (**Figure 6**), and 4 (**Figure 5**) using upwelling winds, temperature, AVHRR, and MURS data before and after the warming event date. Events 1 and 4 (the 1st and 4th largest rapid warming events as defined previously) exhibited the same trends. Inside the bay, noticeable warming occurred following the relaxation of upwelling winds. Following the increase in upwelling winds, temperatures in the bay started to decrease, but not to the same extent as they decreased outside of the bay. The spatial distribution of temperature showed the presence of an upwelling plume that extended across the outer portion of the bay, with warmer waters initially trapped inside the bay.

The initial rapid warming within the embayment, however, was not always evident in the satellite data. Notably, the in-situ temperature data identified an extreme warming event (i.e., > 0.07 ºC/hr) within CPP at both 3 m and 5 m depths, but not outside at DC (**Table 1**).

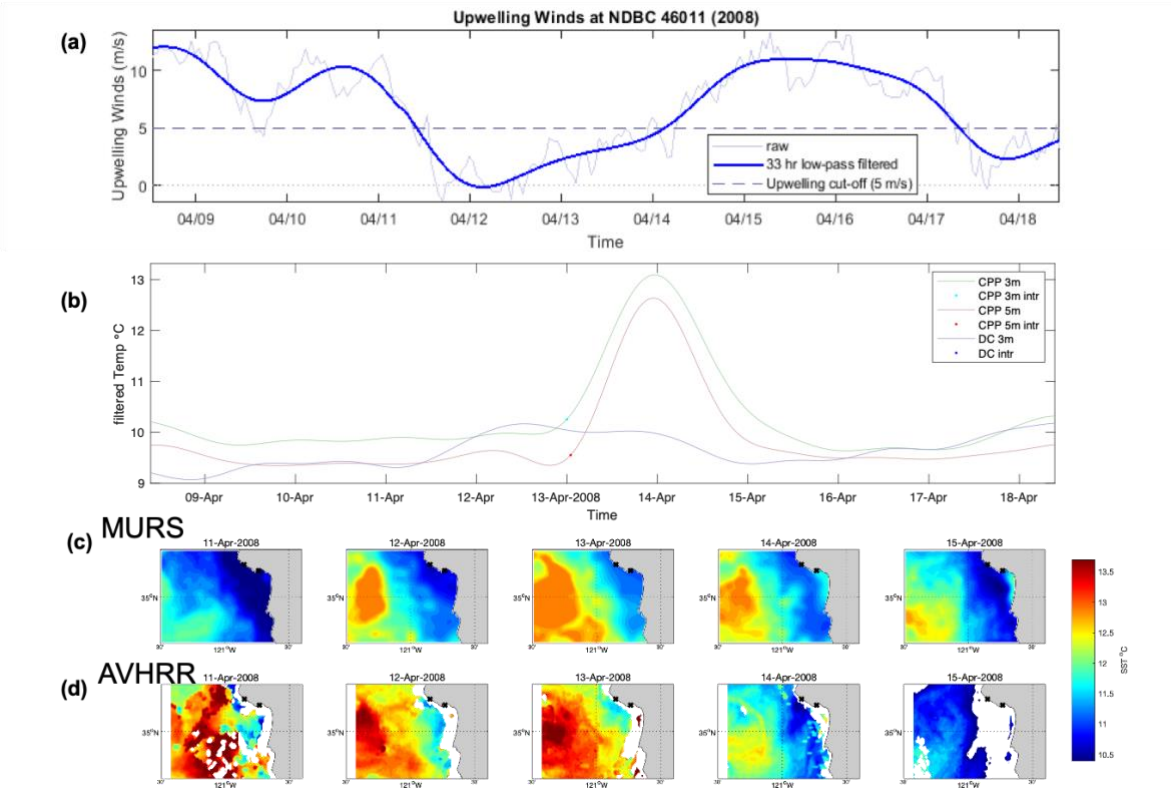

Figure 4. Largest rapid warming event captured at CPP 3 m using a threshold of 0.07 ºC/hr, on April 13th 2008. (a) Upwelling winds. (b) Temperature data for CPP 3 m, 5 m, and DC 3 m for that event (starting date +- 5 days), with dot markers indicating the start of the warming event. (c) MURS and (d) AVHRR data for the starting date +- 2 days. The black markers in (c) and (d) show the locations of CPP (inside bay) and DC (outside bay).

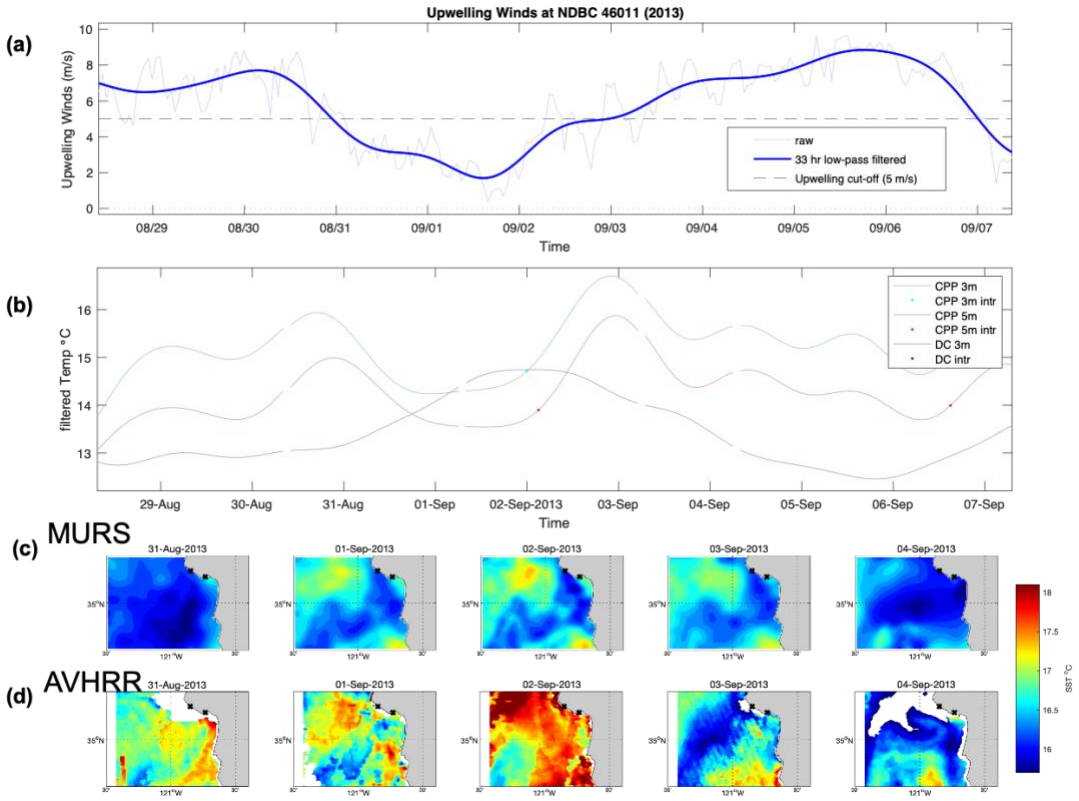

Figure 5. Same as Figure 4, but for the fourth largest rapid warming event on September 2nd 2013.

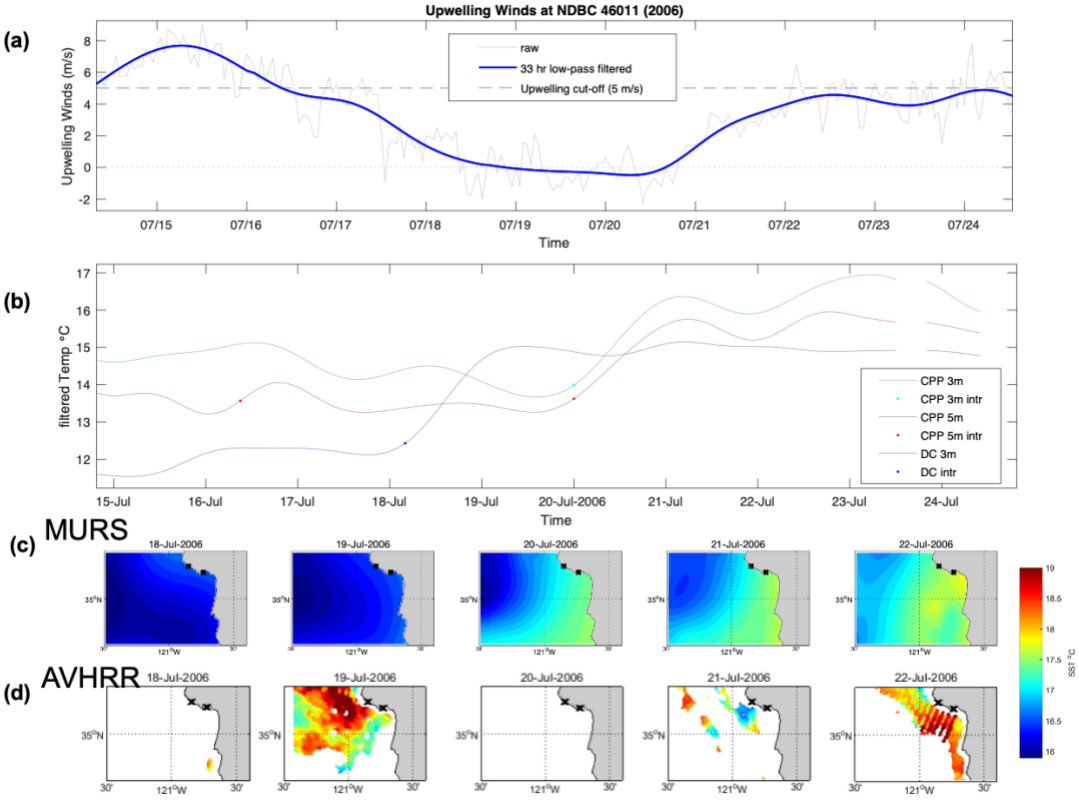

Figure 6. Same as Figure 4, but for the third largest rapid warming event on July 20th 2006.

Event 3 exhibited different trends, as this event occurred both within CPP at both depths, and outside at DC, during a relaxation event (**Table 1**). DC experienced a warming event almost two days before warming occurred in CPP, and then stayed at a consistent temperature as CPP warmed (**Figure 6**)**.** Also, no significant upwelling wind took place after the event, resulting in no noticeable decrease in temperatures after warming, either at CPP or DC. The AVHRR satellite data for this event were spatially sparse, but the MURS data show patterns consistent with a large-scale retreat of warm offshore water during a relaxation event.

Notably, all three events had the common characteristic that warming occurred after a wind relaxation event, exhibiting upwelling-favorable winds that subsided before rapid warming was captured. Overall, similar trends in upwelling winds also resulted in similar temperature changes and trends across all events investigated.

4 Discussion

Based on the overall seasonal trends of the rapid warming events (**Figure 3**), as well as the trends seen for the individual cases observed (**Figures 4-6**), these events are associated with wind relaxation events. All cases detailed exhibited warming approximately 1-3 days after upwelling winds subsided (i.e., relaxation event). However, our data does not indicate a clear source of these warm waters for all cases. One possible mechanism could be the large-scale advection of warm offshore waters displaced by Ekman transport during coastal upwelling, or the poleward propagation of warm waters from south of Point Conception in the form of a buoyant plume front (Washburn et al. 2011; Suanda et al. 2016). Nidzieko and Largier (2013) found that the intrusions may originate as eddies (or their filaments) generated by submesoscale instabilities along the

offshore upwelling front. Future work should further investigate transport pathways using high-frequency radar, as well as the timing of events with respect to upwelling and relaxation cycles.

The increased occurrence of rapid warming events inside the bay may be due to the local coastline orientation and the trapping of warm waters within. When upwelling forcing resumes, the upwelling jet and plume trap waters within the bay, resulting in an upwelling shadow system (**Figure 4**). DC is in direct path of this upwelling plume, while CPP is shielded from it, allowing temperatures to remain higher for a longer period of time inside the bay. Some of the sustained, warm waters within the bay can be seen on April 14th 2008 (**Figure 4**). However, much of the AVHRR SST data, which is not smoothed, was missing. Such an upwelling shadow system may provide a "stepping stone" and an aid for larval dispersal south of Point Conception, which is a major biogeographic boundary. Nidzieko and Largier (2013) found that intrusions due to submesoscale instabilities move southern waters further northward than a typical relaxation plume (e.g., Washburn et al. 2011; Suanda et al. 2016), indicating larval dispersal and connectivity range may be increased due to these intrusions. Additionally, they suspect that upwelling jets may also contribute to onshore transport of warm waters by means of mushroom-like vortices that entrain the warm, offshore waters and bring them onshore. These upwelling jets may even provide more momentum than submesoscale processes, leading to a more significant impact on larval connectivity.

The increased presence of these rapid warming events and intrusions in the bay could also impact local ecology by exposing organisms to more extreme and frequent warming events. Studies performed on the proteomic changes in marine gastropods showed that heat shock proteins can be activated within hours after heat stress begins, and may take 6 hrs or more to return to pre-stress levels (Vasquez et al., 2019). Temperature has also been shown to influence larval dispersal

distance, survival, and development relatively consistently across species, although the effects of increased temperature on recruitment varies between species (O'Connor et al. 2007). Additionally, Safaie et al. (2018) found that coral species frequently exposed to high-frequency temperature variability may protect coral from bleaching due to warming ocean temperatures, as they become more accustomed to higher temperature ranges. Studying whether a similar response is present in kelp forests, an extremely important marine habitat, may help benefit their conservation. Kelp forests along the CA coast have been decimated due to prolonged warming during the recent North Pacific Marine Heatwave (Beas-Luna et al. 2020). Understanding the role that these rapid, but short time-scale, warming events play in kelp forest physiology may provide scientists and managers tools to conserve this critically important habitat as ocean temperatures rise globally. Rapid temperature changes and high temperature variability likely have a significant influence on organisms, and play an important role in shaping local ecosystem response. Understanding how organisms and ecosystems respond to these rapid warming events may provide clues as to how they will respond to expected long-term climate-driven ocean warming and should be considered in future studies.

5 Conclusion

Temperature variability in the nearshore costal ocean influences various biological processes and can drive changes in biodiversity and habitat range. Despite recent progress, there are still significant gaps in the understanding of drivers of temperature variability in upwelling bays, particularly at higher frequencies. In this study, we analyzed a decade of nearshore temperature measurements both inside and outside a small coastal embayment located in central California [San Luis Obispo (SLO) bay], as well as temperature data from satellites, to characterize

rapid warming events. We found that rapid warming events, defined using rates of temperature change across different thresholds, occurred more frequently and with greater magnitudes during the major upwelling season (April to September). Warming events occurred more frequently inside the bay compared to outside, and warmer temperatures were sustained within the bay as a result of an upwelling shadow system, due to the local coastline orientation and topography. The largest warming events typically occurred during a regional upwelling wind relaxation period. The exact source of the warm waters requires further research, but possible sources include the large-scale advection of offshore waters during relaxation events, the poleward propagation of warm waters as a buoyant plume front during relaxation events, and/or eddies and filaments generated by submesoscale instabilities. These rapid warming events could have a significant influence on the physiology of nearshore organisms and the connectivity of larvae. Further investigation into how organisms and ecosystems respond to these rapid warming events may provide insight into how they will respond to climate-driven ocean warming, with important conservation implications.

6 Acknowledgements

We acknowledge support from the NOAA IOOS program through CeNCOOS for the data collected at the Cal Poly Pier, as well as PIs and technicians that helped maintain these systems, especially Ian Robbins. We also acknowledge John Steinbeck at Tenera Environmental for providing us with the DC temperature data. Finally, I am extremely grateful to my advisor, Dr. Ryan Walter, for his invaluable mentorship, guidance, and support throughout my past four years doing research in his lab, and for allowing me the opportunity to work on this project. The irreplaceable experiences and skills I have obtained working for him will continue to serve me throughout my future career and research efforts.

References

Barth, A., Walter, R.K., Robbins, I., Pasulka, A., 2020. Seasonal and interannual variability of phytoplankton abundance and community composition on the Central Coast of California. Mar. Ecol. Prog. Ser. 637:29-43. https://doi.org/10.3354/meps13245

Beas-Luna, R., Micheli, F., Woodson, C.B., Carr, M., Malone, D., Torre, J., Boch, C., Caselle, J.E., Edwards, M., Freiwald, J., Hamilton, S.L., Hernández, A., Konar, B., Kroeker, K.J., Lorda, J., Montaño-Moctezuma, G., Torres-Moye, G., 2020. Geographic variation in responses of kelp forest communities of the California Current to recent climatic changes. Global Change Biology. 26, 1-17. https://doi.org/10.1111/gcb.15273

Booth, J.A.T., McPhee-Shaw, E.E., Chua, P., Kingsley, E., Denny, M., Phillips, R., Bograd, S.J., Zeidberg, L.D., Gilly, W.F., 2012. Natural intrusions of hypoxic, low pH water into nearshore marine environments on the California coast. Continental Shelf Research. 45, 108-115. https://doi.org/10.1016/j.csr.2012.06.009

Lucas, A.J., Franks, P.J.S., Dupont, C.L., 2011. Horizontal internal-tide fluxes support elevated phytoplankton productivity over the inner continental shelf. Limnology and Oceanography: Fluids and Environments. 1, 56-74. https://doi.org/10.1215/21573698-1258185

Chavez, F.P., Messié, M., Pennington, J.T., 2011. Marine primary production in relation to climate variability and change. Ann. Rev. Mar. Sci. 3, 227–260. https://doi.org/10.1146/annurev.marine.010908.163917

Garcia-Reyes, M., Largier, J.L., 2012. Seasonality of coastal upwelling off central and northern California: New insights, including temporal and spatial variability. J. Geophys. Res. Oceans 117, n/a n/a. https://doi.org/10.1029/2011JC007629

Largier, J.L., 2020. Upwelling Bays: How Coastal Upwelling Controls Circulation, Habitat, and Productivity in Bays. Annu. Rev. Mar. Sci. 12, 415–447. https://doi.org/10.1146/annurev-marine-010419-011020

Melton, C., Washburn, L., Gotschalk, C., 2009. Wind relaxations and poleward flow events in a coastal upwelling system on the central California coast. J. Geophys. Res. Oceans 114, C11016. https://doi.org/10.1029/2009JC005397

Nidzieko, N.J., Largier, J.L., 2013. Inner shelf intrusions of offshore water in an upwelling system affect coastal connectivity. Geophys. Res. Lett. 40, 5423-5428. https://doi:10.1002/2013GL056756

O'Connor, M.I., Bruno, J.F., Gaines, S.D., Halpern, B.S., Lester, S.E., Kinlan, B.P., Weiss, J.M., 2007. Temperature control of larval dispersal and the implications for marine ecology, evolution, and conservation. Proceedings of the National Academy of Sciences, 104 (4), 1266-1271. https://doi.org/10.1073/pnas.0603422104

Paduan, J.D., Cook, M.S., Tapia, V.M., 2018. Patterns of upwelling and relaxation around Monterey Bay based on long-term observations of surface currents from high frequency radar. Deep Sea Research Part II: Topical Studies in Oceanography, 151, 129-136, https://doi.org/10.1016/j.dsr2.2016.10.007.

Safaie, A., Silbiger, N.J., McClanahan, T.R., Pawlak, G., Barshis, D.J., Hench, J.L., Rogers, J.S., Williams, G.J., Davis, K.A., 2018. High frequency temperature variability reduces the risk of coral bleaching. Nat. Commun. 9, 1671. https://doi.org/10.1038/s41467-018-04074-2

Suanda, S.H., Kumar, N., Miller, A.J., Di Lorenzo, E., Haas, K., Cai, D., Edwards, C.A., Washburn, L., Fewings, M.R., Torres, R., Feddersen, F., 2016. Wind relaxation and a coastal buoyant plume north of Pt. Conception, CA: Observations, simulations, and scalings. J. oGeophys. Res. Oceans, 121, 7455-7475. https://doi.org/10.1002/2016JC011919

Valera, M., Walter, R.K., Bailey, B.A., Castillo, J.E., 2020. Machine Learning Based Predictions of Dissolved Oxygen in a Small Coastal Embayment. J. Mar. Sci. Eng., 8, 1007. https://doi.org/10.3390/jmse8121007

Vasquez, M.C., Lippert, M.R., White, C., Walter, R.K., Tomanek, L., 2019. Proteomic changes across a natural temperature gradient in a marine gastropod. Marine Environmental Research, 149, 137-147. https://doi.org/10.1016/j.marenvres.2019.06.002

Walter, R.K., 2018. Coastal upwelling seasonality and variability of temperature and chlorophyll in a small coastal embayment. Continental Shelf Research, 154, 9-18. https://doi.org/10.1016/j.csr.2018.01.002

Walter, R.K., Stastna, M., Woodson, C.B., Monismith, S.G., 2016. Observations of nonlinear internal waves at a persistent coastal upwelling front. Continental Shelf Research, 117, 100-117. https://doi.org/10.1016/j.csr.2016.02.007

Walter, R.K., Reid, E.C., Davis, K.A., Armenta, K.J., Merhoff, K., N. J. Nidzieko, N.J., 2017. Local diurnal wind-driven variability and upwelling in a small coastal embayment. J. Geophys. Res. Oceans, 122, 955–972. https://doi:10.1002/2016JC012466

Walter, R.K., Woodson, C.B., Arthur, R.S., Fringer, O.B., Monismith, S.G., 2012. Nearshore internal bores and turbulent mixing in southern Monterey Bay. J. Geophys. Res. 117, C07017. https://doi.org/10.1029/2012JC008115

Walter, R.K., Woodson, C.B., Leary, P.R., Monismith, S.G., 2014. Connecting wind-driven upwelling and offshore stratification to nearshore internal bores and oxygen variability. J. Geophys. Res. Oceans, 119, 3517– 3534. https://doi.org/10.1002/2014JC009998

Washburn, L., Fewings, M.R., Melton, C., Gotschalk, C., 2011. The propagating response of coastal circulation due to wind relaxations along the central California coast. J. Geophys. Res. Ocean. 116. http://dx.doi.org/10.1029/2011JC007502

Wolanski, E., Pickard, G.L., Jupp, D.L.B., 1984. River plumes, Coral Reefs and mixing in the Gulf of Papua and the northern Great Barrier Reef. Estuarine, Coastal and Shelf Science, 18, Issue 3, 291-314. https://doi.org/10.1016/0272-7714(84)90073-8